

Electrical Resistivity Tomography across the Paganica-San Demetrio fault system (L'Aquila 2009 earthquake)

A. GIOCOLI¹, P. GALLI^{2,3}, B. GIACCIO³, V. LAPENNA¹, P. MESSINA³, E. PERONACE¹, G. ROMANO¹ and S. PISCITELLI¹

¹ Institute of Methodologies for Environmental Analysis, CNR, Tito Scalo (PZ), Italy

² Civil Protection Department, Rome, Italy

³ Institute of Environmental Geology and Geoengineering, CNR, Rome, Italy

(Received: May 21, 2010; accepted: November 15, 2010)

ABSTRACT The M_w 6.3, 2009 earthquake (L'Aquila, central Italy) was characterized by discontinuous surface rupture along the 19-km long NW-SE trending Paganica-San Demetrio fault system. The earthquake nucleated just below the town of L'Aquila at a depth of ca. 9 km, rupturing mainly toward SE. Due to the high urbanization of the area and to centuries-long agricultural works, the surficial traces of this fault system are not clear everywhere. In order to provide more detailed and accurate information concerning the Paganica fault segment, four Electrical Resistivity Tomographies (ERT) were carried out around the Paganica village area. ERT results were supported by interpretation of aerial photos, morphotectonic investigation, geological field survey, borehole data and a paleoseismological trench. The electrical images showed the cumulated offset of the fault at depth and the existence of other splays parallel to the main strand which depict a staircase geometry of the fault in the Paganica area.

Keywords: ERT, Paganica-San Demetrio fault system, April 6, 2009 L'Aquila earthquake, central Italy.

1. Introduction

On April 6, 2009, a moderate earthquake (M_w 6.3, depth about 9 km) struck the L'Aquila region (central Apennines, Italy), awakening also millions of citizens in the city of Rome, 100-km away. The earthquake nucleated just below the town of L'Aquila, rupturing toward SE as suggested by instrumental (Cirella *et al.*, 2009) and macroseismic data (Galli *et al.*, 2009). The focal mechanisms of the main event yields NW-striking normal faulting (Pondrelli *et al.*, 2009), matching the ~ 19 km long, NW-SE trending and SW-dipping Paganica-San Demetrio normal fault system [PSDFS: Boncio *et al.* (2010) and Galli *et al.* (2010)]. The PSDFS is built up by five main 1-to-5 km long fault strands that are arranged in a right-stepping *en-echelon* pattern, namely (from NW to SE; Fig. 1) the La Serra-Colle Enzano fault (SCE), the Colle della Capanna fault (CCF), the Paganica fault (PF), the San Gregorio fault (SGF) and the San Demetrio fault (SDF) (Galli *et al.*, 2010). Surficial breaks due to coseismic fault rupture were observed along its entire length, with a maximum vertical offset of 10-15 cm (Falcucci *et al.*, 2009; Boncio *et al.*, 2010; Galli *et al.*, 2010).

In spite of the numerous geological studies carried out in this sector of the central Apennines

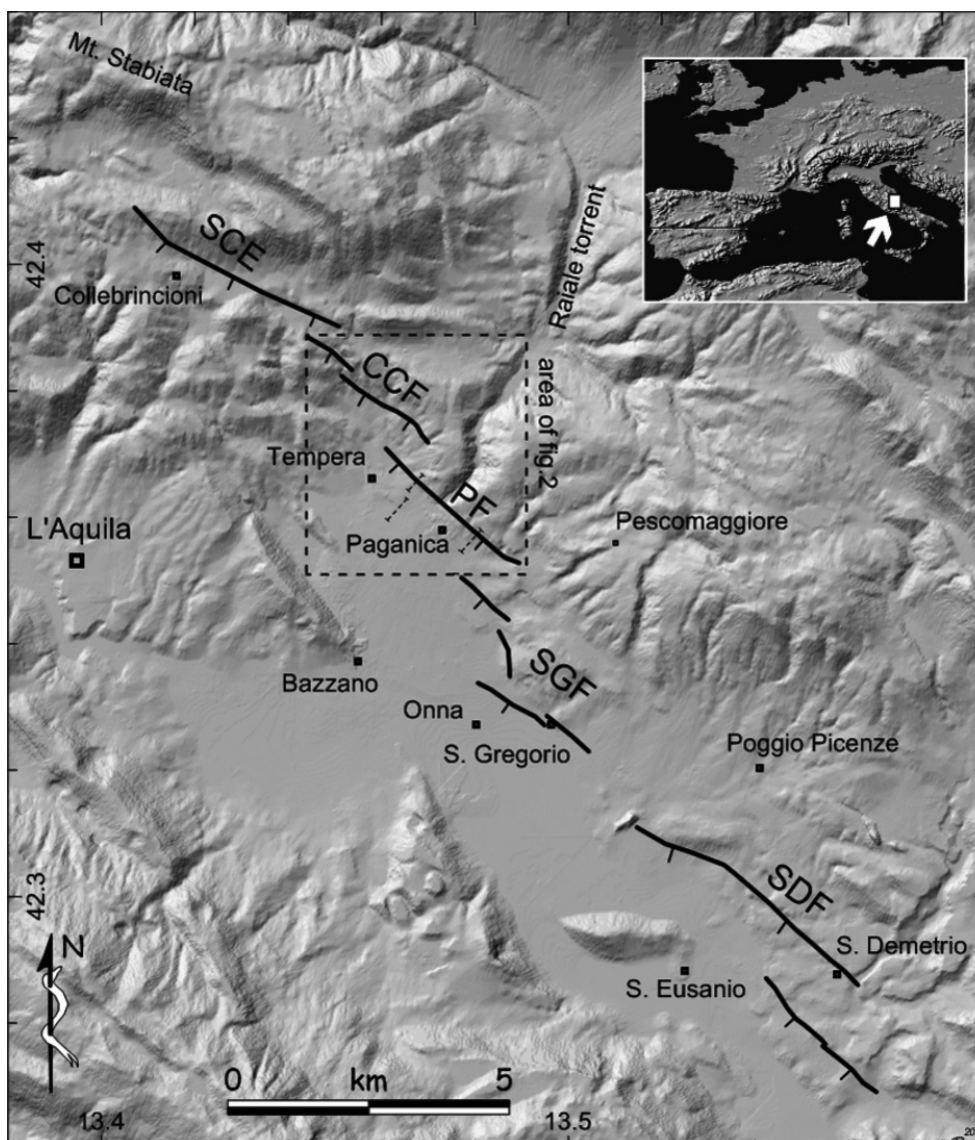


Fig. 1 - Map of the Paganica-San Demetrio fault system: La Serra-Colle Enzano fault (SCE); Colle della Capanna fault (CCF); Paganica fault (PF); San Gregorio fault (SGF) and San Demetrio fault (SDF).

(e.g., Bosi, 1975; Galadini and Galli, 2000; Boncio *et al.*, 2004, and references therein), the PSDFS has been hitherto a poorly known structure within the L'Aquila fault system, not only in terms of its general geometry but also concerning the age of the affected Quaternary successions. This was also due to the high urbanization of the area and to the centuries-long agricultural works, which hampered the correct identification of the fault, erasing in some places the surficial trace of the fault itself.

In this work, we present the results of a high-resolution Electrical Resistivity Tomography (ERT) survey carried out around the Paganica village. Our investigations were aimed at the

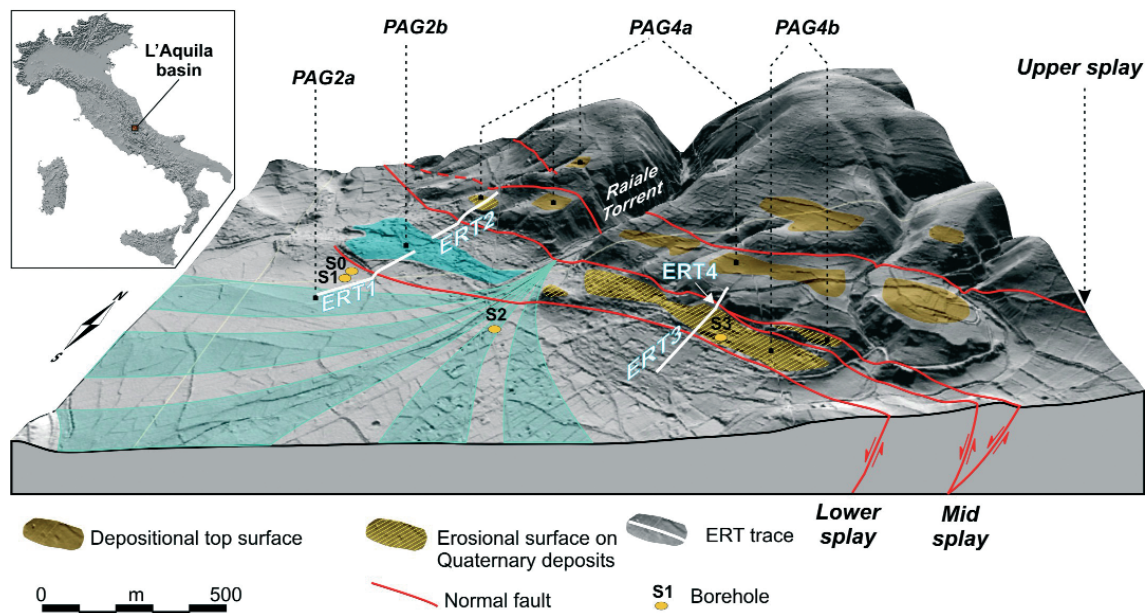


Fig. 2 - 3D surface-DEM (1-m spaced grid; from Lidar data) of the Paganica area and the superimposed map of the main outcropping morpho-sedimentary units and fault traces. Location of the ERT profiles and boreholes are also shown. Note that the ERT4 profile coincides with the location of a paleoseismological trench [see details in Galli *et al.* (2010)].

definition of the Paganica fault geometry, and at establishing the link with the morphological and stratigraphical framework proposed by Galli *et al.* (2010). The analyses put in evidence the fact that the Paganica fault segment consists of at least three sub-parallel main splays, here labelled as upper, mid and lower (UPF, MPF and LPF), which have a normal fault staircase geometry in the investigated area.

2. Geological and geomorphological framework

Integrated morphological, stratigraphical and structural investigations allowed us to recognize seven main depositional and pedogenetic units and three main sub-parallel and synthetic fault splays around the village of Paganica (Messina *et al.*, 2009a, 2009b; details in Galli *et al.*, 2010) (Fig. 2).

The depositional and pedogenetic units are numbered here from the oldest as Paganica-7 to the most recent as Paganica-1. These are separated by erosional surfaces, and are displaced by fault planes at different elevations on the present Raiale talweg. Some units also showed well-preserved, terraced, depositional top surfaces that provided a further distinguishing element for their identification throughout wide sections of the area. A distinctive paleosol horizon and some tephra layers were also used as stratigraphic markers.

The seven units are related to different depositional systems and environments, including: lacustrine, fluvial, alluvial, colluvial and pedogenetic. The lithological characteristics and

microprobe chemical analyses performed on handpicked fresh glass shards from four tephra layers allowed Galli *et al.* (2010) to correlate them to well-dated ash layers, deriving from the explosive activity of the Colli Albani and Sabatini volcanoes (i.e., Tufo Pisolitico di Trigatoria, TPT, ~560 ka; Pozzolane Rosse, PR, ~456 ka; Tufo Rosso a Scorie Nere, TRSN, ~450 ka; Tufo di Villa Senni, TVS, ~360 ka). By using the four tephra markers for the definition of the local stratigraphy, Galli *et al.* (2010) proposed the following chronological and stratigraphical framework: Paganica-7 (Pag7), fluvial conglomerate older than 780 ka; Paganica-6 (Pag6: 800-560 ka), paleosol; Paganica-5 (Pag5: ca. 560 ka), colluvial deposits; Paganica-4 (Pag4: 550-350 ka), stratified layers of well-sorted and rounded gravels (Pag4a) and massive-to-stratified sand, brownish pedogenic horizons and decimetric-thick layers of rounded gravels (Pag4b); Paganica-3 (Pag3: 300-200 ka), paleosol; Paganica-2 (Pag2: 110-11 ka), alluvial fan gravel that originates from the Raiale Torrent, which shows its original morphology (Pag2a) and well-stratified layers of gravels associated with a wide-terrace barely suspended on the present talweg (ca. 5 m), recognisable in the north-western sector of the Paganica village (Pag2b); Paganica-1 (Pag1: Holocene), colluvial and slope-derived deposits. In addition to these pedo-sedimentary units, Galli *et al.* (2010) recognised two main erosional phases occurring in between Pag7 and Pag6, and Pag3 and Pag2, and therefore dated according at ca. 800-660 ka and 200-110 ka, respectively.

The depositional top surface of the Pag4 unit is at an elevation of 820 m a.s.l. west of Pescomaggiore; NE of Paganica, the same surface was found at 740 m a.s.l.. The different elevation at which we surveyed this geomorphic surface is due to the displacement of the UPF which throws the paleofan succession down SW-wards (Fig. 2). In some places, this splay puts the Meso-Cenozoic bedrock (massive limestone, stratified limestone, marly limestone, calcareous marls, marls, etc.) directly in contact with the alluvial deposits, dragging also the Tufo Pisolitico di Trigatoria tephra along the shear plane. The entire succession is further thrown down by the MPF and the LPF, which are characterized by rectilinear rock scarps over which the outskirts of Paganica have been founded. The scarps are carved into the conglomerate of the Pag7 unit, and most of the surficial breaks of April 2009 were observed along them. Finally, towards SW, the uppermost part of the fluvial succession of the Pag4 unit (i.e., sands containing the Tufo di Villa Senni tephra, 680 m a.s.l.) is definitely lowered below the present alluvial plain by the LPF, even though its surface expression is not clear everywhere. Nevertheless, SE of Paganica a rectilinear scarp is still visible amongst the buildings, while west of Paganica, at ~650 m a.s.l., another NW-SE oriented scarp facing SW runs across the present Raiale fan surface. Since these scarps are perpendicular to the strike of the main streams, it is quite difficult to explain their nature by linear erosion processes. Therefore, we suspect that they represent the surface expression of the LPF splay.

In order to unravel this uncertainty, the existence of the LPF and the MPF has been explored both SE and west of Paganica through different ERT profiles. In all cases, the suspected fault trace at depth has been put in evidence by abrupt vertical resistivity anomalies, fitting at the surface with the aforementioned morphological indications. This interpretation is confirmed by the analyses of trenches and borehole logs collected in the area (see the stratigraphy of three boreholes - S0, S2, S3 - in Fig. 3) which have put in evidence a staircase geometry of the Meso-Cenozoic bedrock.

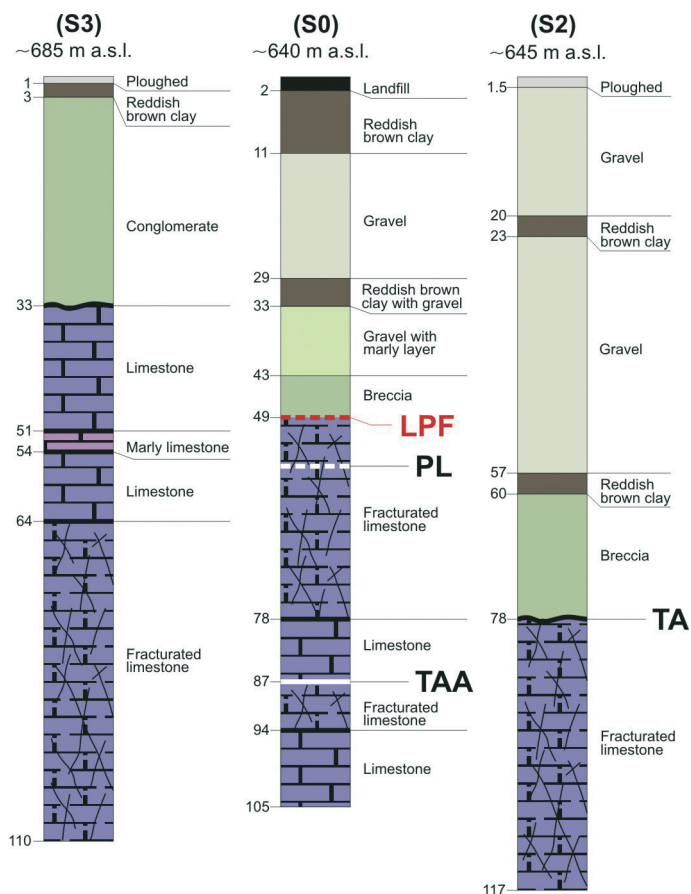


Fig. 3 - Three borehole logs used to infer the geometry of the bedrock and of the sediment cover across the LPF splay. TA - top aquifer; TAA - top of the artesian aquifer; PL - piezometric level. See Fig. 2 for the location of each borehole.

3. Electrical resistivity tomography survey

The ERT method is a fast, non-invasive and low cost geophysical method, widely applied to obtain 2D high-resolution images of the subsurface resistivity pattern. It has proven to be useful in providing the exact location and the structural characteristics of faults (e.g., *Giano et al.*, 2000; *Storz et al.*, 2000; *Suzuki et al.*, 2000; *Demanet et al.*, 2001; *Caputo et al.*, 2003, 2007; *Wise et al.*, 2003; *Nguyen et al.*, 2005; *Galli et al.*, 2006; *Giocoli et al.*, 2008a; *Improta et al.*, 2010), to infer some characteristics of the fault zones, such as the presence of fluids (*Siniscalchi et al.*, 2010), to estimate the width of the damage zone (*Diaferia et al.*, 2006) and to delineate the structural setting of geological sedimentary basins (*Rizzo et al.*, 2004; *Giocoli et al.*, 2008b).

In this work, the ERT method was employed to investigate the Paganica fault at three sites (ERT1, ERT2 and ERT3 - see Fig. 2) around the Paganica village. All surveys were aimed at: 1) interpreting the nature of the geomorphological features observed at the surface, 2) detecting and pinpointing fault location, 3) characterizing the structure of the fault zone, 4) estimating the cumulative displacement and 5) establishing the best emplacement for later paleoseismological trenches.

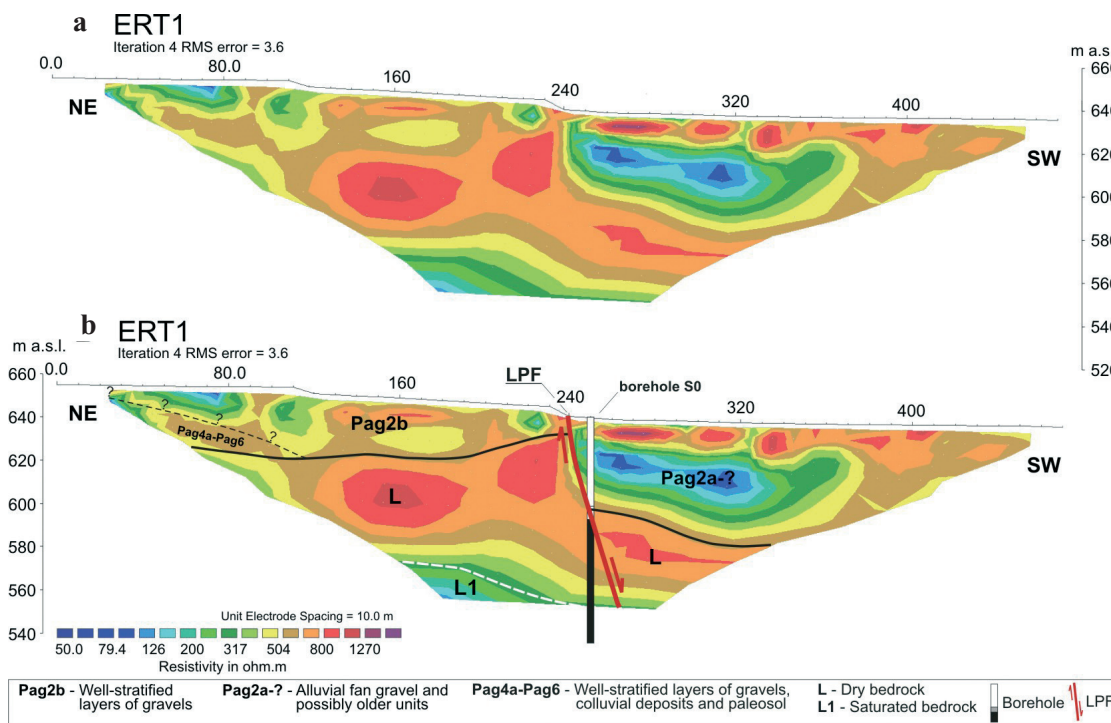


Fig. 4 - ERT1 (a) carried out across the LPF splay (see Fig. 2 for location) and its interpretation (b).

The ERT surveys were performed by means of a Syscal R2 (Iris Instruments) resistivity meter, coupled with a multielectrode acquisition system (46 or 48 electrodes). A constant spacing “*a*” (1 or 10 m) between adjacent electrodes was used. Along each profile, we applied different array configurations (Wenner-Schlumberger and Dipole-Dipole) and different combinations of dipole length (1a, 2a and 3a) and “*n*” number of depth levels ($n \leq 6$), obtaining investigation depths of about 10 m (for $a = 1$ m) and 100 m (for $a = 10$ m).

The Wenner-Schlumberger and Dipole-Dipole apparent resistivity data were inverted using the RES2DINV software (Loke, 2001) to obtain the 2D resistivity images of the subsurface. In all cases, the best result was obtained from the Wenner-Schlumberger data which have shown a higher signal-to-noise (s/n) ratio, a larger investigation depth and a better sensitivity pattern to both horizontal and vertical changes in the subsurface resistivity. The Root Mean Squared (RMS) error was less than 5% and the resistivity values range from 50 to more than 1270 Ωm .

Thanks to the data gathered through geological surveys, trench-analyses, exploratory boreholes and aerial photo interpretations, we were able to calibrate the ERT results and to directly correlate resistivity values with the lithostratigraphic characteristics. In general, the lowest resistivity values ($\rho < 250 \Omega\text{m}$) correspond to saturated bedrock or sand-gravel deposits with thin paleosol levels at the bottom (Pag1, Pag2a, Pag3, Pag4b, Pag5 and Pag6), while the highest measured resistivity values ($\rho > 250 \Omega\text{m}$) are associated with dry bedrock, conglomerate and well-sorted gravels (Pag7, Pag4a and Pag2b). Resistivity is, therefore, extremely variable

from formation to formation, and even within a particular formation.

3.1. ERT1

West of the Paganica village, a NW-SE scarp facing SW-wards runs across the present Raiale fan surface. This scarp is perpendicular to the strike of the main streams, so we suppose it might represent the surficial expression of the LPF splay. In order to verify the nature of the scarp observed at surface and to interpret it either as a tectonic landform (i.e., fault scarp) or as a geomorphic feature (i.e., erosional scarp), an ERT survey (ERT1 in Fig. 2) was performed. Here, we used a 48-multielectrode acquisition system with 10 m of electrode spacing, which allowed us to reach a depth of about 100 m along the 470-m long ERT1 (Fig. 4a). In particular, the ERT1 profile runs NE-SW on both Pag2a and Pag2b units. The scarp is crossed at about 240 m.

The interpretation of the ERT1 is supported by both surface and borehole data (S0 in Fig. 3), and is shown in Fig. 4b.

In the upper part of the tomography, between 0 - 240 m, the moderate resistivity values can be related to Pag2b, probably laying on top of the paleo-Raiale deposits (Pag4a-Pag6 units) in the northernmost sector. Between 240 - 470 m, the low-moderate resistivity values can be associated to Pag2a and possibly older units. All along the ERT2, the Raiale deposits cover the Meso-Cenozoic bedrock (L), which is characterized by the highest resistivity values. At the bottom, the decrease in the resistivity values of the bedrock, at depths greater than about 85 m, is associated to the presence of an artesian aquifer, as testified by borehole S0 (Fig. 3). Through borehole S0, the groundwater was able to rise (about 31 m - PL in Fig. 3) above the level where it was first encountered (about 87 below the ground surface - TAA in Fig. 3).

The major feature of the ERT1 is the sharp lateral variation of resistivity at about 240 m which fits precisely with the mentioned scarp observed at the surface. This feature is correlated with the LPF observed in the S0 borehole at 49 m depth (LPF in Fig. 3). Thus, we can speculate that the morphological indication (scarp) is the surficial expression of the LPF splay that throws the base of the Raiale deposits at least 35 m down SW-wards (Figs. 4a and 4b).

3.2. ERT2

During the April 6 earthquake, NW of Paganica downtown, a strong jet of water, generated by a leak in the Gran Sasso Aqueduct, dug a deep, rectilinear, 50-m long gorge within the Pleistocene sedimentary succession. This impressive feature exposed along its walls alluvial and slope deposits displaced across at least three shear planes. These are the surficial features of the 30-m wide MPF fault zone [see details in Falcucci *et al.* (2009), Boncio *et al.* (2010) and Galli *et al.* (2010)].

In order to image the architecture of the fault zone at depth, we carried out a 450-m long ERT (ERT2) along the aqueduct trench, using a 46-multielectrode acquisition system with an electrode spacing of 10 m and an investigation depth of about 95 m. The ERT2 is situated about 90 m upslope and on the continuation of the NE-SW ERT1 profile (see Fig. 2). The ERT1 and ERT2 profiles were not combined in a single long profile, by applying a roll-along acquisition method, due to logistical conditions (i.e., presence of main road and buildings).

The ERT2 profile crosses the Pag4a and La units (see Figs. 2 and 5) on the surface. Fig. 2 shows also that the upslope part of ERT1 is situated on an erosional surface which cuts the Pag4a

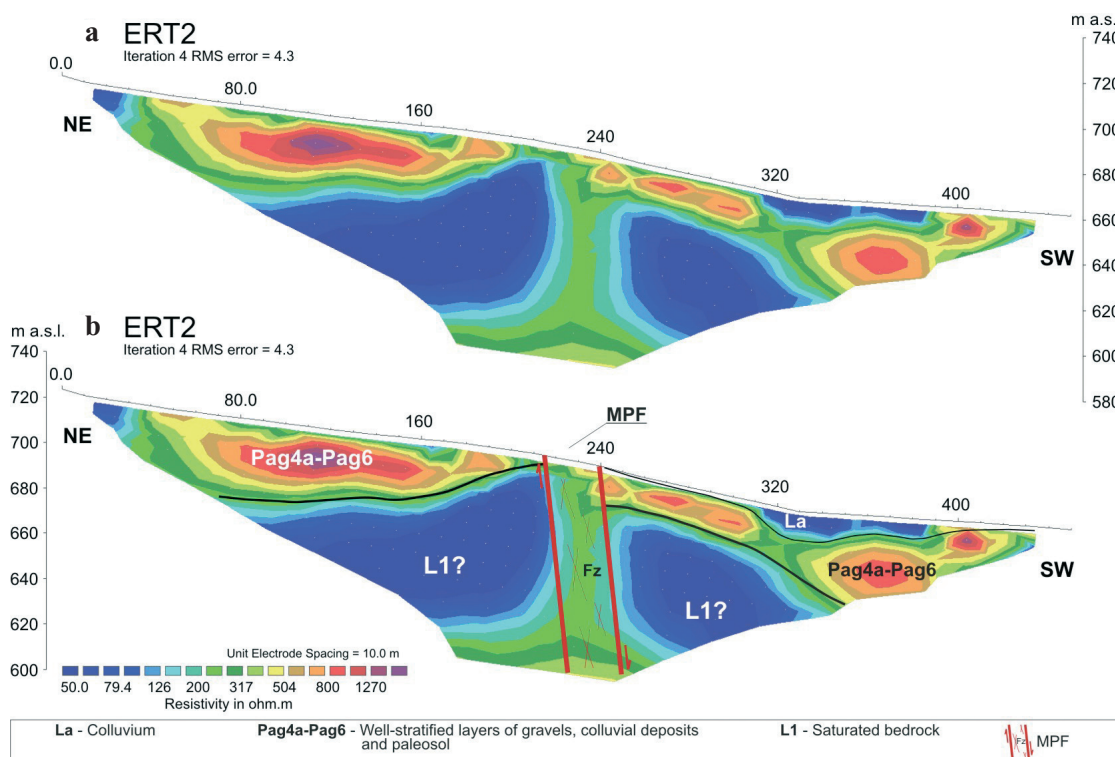


Fig. 5 - ERT2 (a) carried out across the MPF splay (see Fig. 2 for exact location) and its interpretation (b).

unit. The MPF fault zone, observed in the aqueduct gorge, is located between 210 - 240 m along the ERT2 profile. In this case, there are no borehole data that could aid in constraining the interpretation of ERT2. However, considering that ERT1 and ERT2 are so close, it is possible to interpret the ERT2 on the basis of the data coming from both ERT1 and the borehole (S0 in Figs. 2 and 3).

The electrical image of ERT2 is shown in Fig. 5a, while its geological interpretation is presented in Fig. 5b.

In the upper part of ERT2, where the ERT2 profile crosses the erosional surface, high resistivity values ($\rho > 250 \Omega\text{m}$) can be associated to the Pag4a unit which gently thickens NEwards, from about 5 to 35 m of thickness. In the middle, relatively low resistivity values ($\rho < 250 \Omega\text{m}$) could be related to the saturated bedrock (unit L) which has been also observed in ERT1 and in the borehole S0 (at depths greater than 87 m). The central resistivity zone (sector Fz), which shows moderate values (about $300 \Omega\text{m}$), matches the $\sim 30\text{-m}$ wide impermeable fault-zone observed in the aqueduct gorge. According to ERT2, the vertical offset of the top of the inferred bedrock is ca. 20-25 m. At the bottom, the electrical image shows an increase in resistivity values that could be due to a change in hydrogeological conditions (i.e., variations in water content) and/or local change in bedrock lithology, from marly limestone-to-limestone.

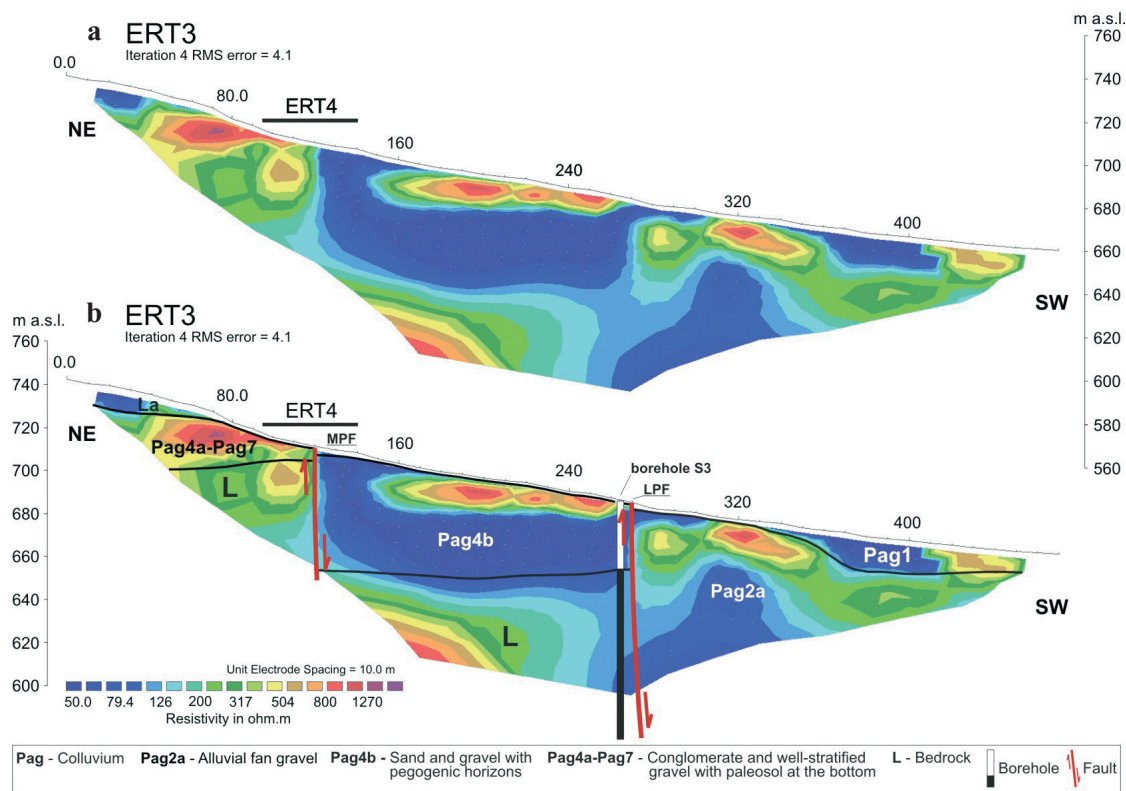


Fig. 6 - ERT3 (a) carried out across the LPF and MPF splays (see Fig. 2 for location) and its interpretation (b).

3.3. ERT3-4

About 1.3 km SE of ERT1 and ERT2, we pinpointed a third site-test for ERT analysis (see Fig. 2) across the possible traces of the MPF and LPF splays of the Paganica fault. Here, we carried out two overlapping ERT surveys with different electrode spacing (1 and 10 m) and corresponding depth of investigation (ca. 10 and 100 m) using a 48-multielectrode acquisition system along a straight NE-SW profile.

The 470-m long, ERT3 profile runs across a minor alluvial fan that covers the Pag4a-Pag7 units (NE sector), an erosional surface that cuts the Pag4a units and the colluvium of the Pag1 unit in the south-western outskirts of the Paganica village (Fig. 6a).

The interpretation of the ERT3 is supported by both surface and borehole data (S3 in Figs. 2 and 3), and it is sketched in Fig. 6b.

The resistivity values lower than 250 Ωm could be indicative of different kinds of sand and gravel deposits (Pag1, Pag2a and Pag4b units in Fig. 6b), whereas resistivity values higher than 250 Ωm could be related both to bedrock and well-sorted gravels on conglomerate (L and Pag4a-Pag7 units in Fig. 6b). A valuable constraint on the depth of the bedrock is given by S3 borehole data, showing the bedrock (unit L) overlain by 33-m thick sand and gravel with pedogenic horizons (Pag4b) in the block between MPF and LPF. Thus, the relatively low resistivity zone ($\rho < 250 \Omega\text{m}$), between 120 and 270 m, is interpreted as matching the Pag4b unit, whereas the high-

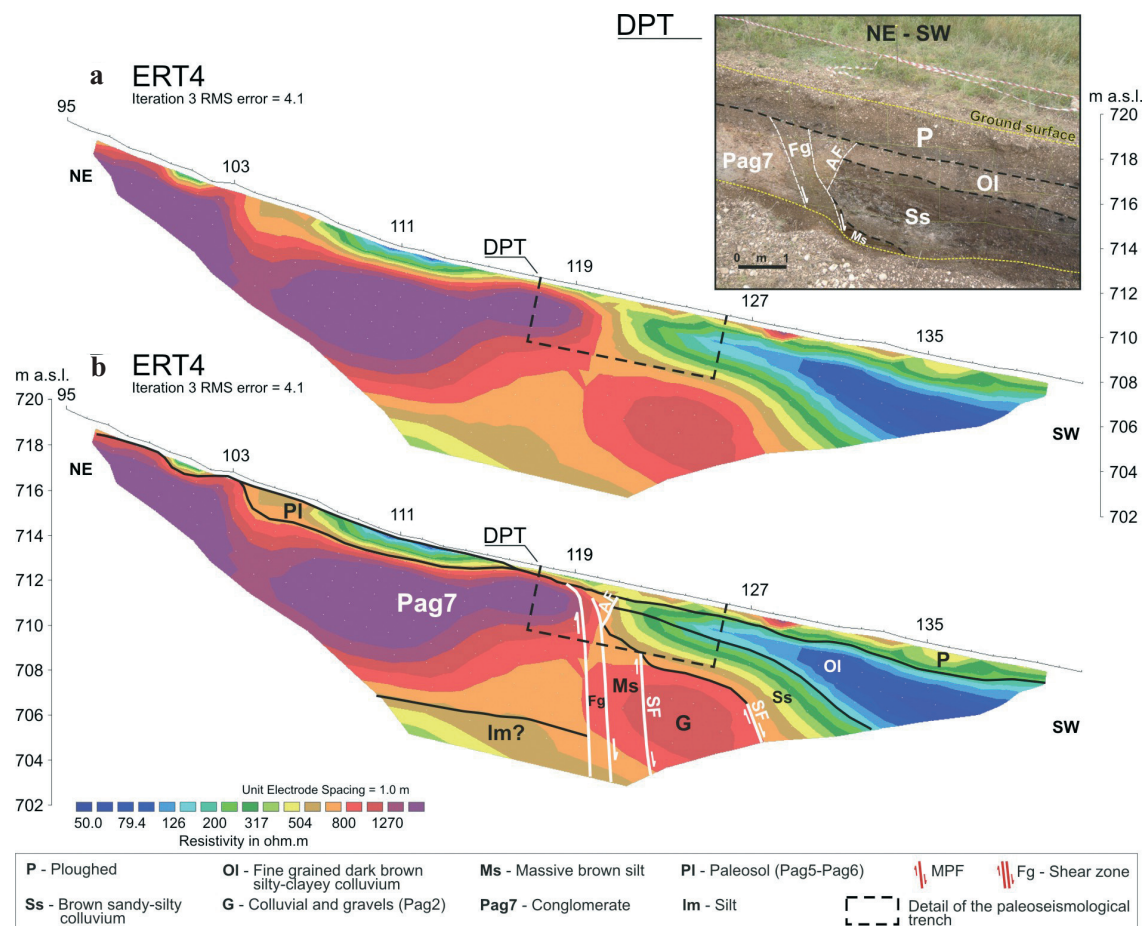


Fig. 7 - High-resolution ERT4 (a) carried out across the MPF overlapping the ERT3 profile between 95 and 142 m (see location in Figs. 2 and 6), detail of the paleoseismological trench (DPT) and interpretation of the ERT4 (b).

moderate resistivity zone ($\rho > 250 \Omega\text{m}$), located at an elevation between about 650 m to more than 600 m a.s.l., is related to bedrock (unit L). In the NE sector of the ERT3, between 0 and 120 m, the presence of a shallow bedrock (from about 5 to maximum 35 m below the ground surface) overlain by well-sorted gravels and conglomerate with paleosol horizon (Pag4a-Pag7) may be inferred in agreement with field geological observation. Conversely, ERT3 does not allow us to infer the existence of the bedrock in the SW sector (e.g., between 270 and 470 m). Here, a thin colluvial cover (unit Pag1) lies directly on the Pag2a deposits. The shallowest high resistivity zones, between 150 and 470 m, are interpreted as filling materials and building foundations which were observed in the field.

From a structural viewpoint, in the central (at about 270 m) and northern sectors (at about 120 m) of ERT3, two sharp lateral resistivity variations are observed and they can be interpreted as the traces at depth of the MPF and LPF, respectively. At least 45 m of cumulative vertical

displacement of the top of the inferred bedrock can be estimated on the MPF.

The second 47-m long ERT4 (electrode spacing of 1 m, see Fig. 7) crossed the apex of the small alluvial fan and overlaps ERT3 between 95 and 142 m. The very high-resolution ERT4 was specifically designed to investigate the MPF and, in particular, to provide details on the very shallow architecture (<10 m depth) of the fault-zone and to evaluate the best siting for a paleoseismological trench.

The very high-resolution ERT4 confirms the same lateral resistivity variation observed in ERT3 at about 120 m. This feature is interpreted as proving the existence of the MPF. In addition, the improved spatial resolution of the ERT4 better constrains the uppermost part of the MPF fault zone between 118 and 123 m and displays new details on architecture of this splay. Thus, a 35-m long, approximate 2.5-m large and maximum 6-m deep, NE-SW-oriented trench was dug along the ERT4 profile between 104 and 139 m [Fig. 7; i.e., the one described in Galli *et al.* (2010)]. Trench data documented that the MPF corresponds to the horizontal variation of resistivity between 118 and 123 m in ERT4 and yielded further valuable constraints for the interpretation of the resistivity model. In particular, the comparison between the ERT4 and trench-logging allowed us to directly correlate resistivity values with the lithostratigraphic characteristics. Successively, the trench data were extended outside the trench-boundary, merely taking into account the ERT4. Thus, the accurate architecture of the MPF fault zone, the shape, the geometry and thickness changes of the most recent sediments were shown in the very near-surface (within the first 10 m, Fig. 7). In all, it was possible to show the high-resistivity conglomerate (Pag7) faulted against a well-stratified succession of low-moderate resistivity slope deposits (Ol, Ss, G and Ms). The deformation was expressed by an about 1-m wide shear zone (Fg) filled with clay material derived from the tephra-rich level (Pag6) layered between the Pag4a and Pag7 units, and by high-angle synthetic (i.e., SF in Fig. 7) and antithetic normal faults (i.e., AF in Fig. 7). Detailed trench-logging and ¹⁴C dating of samples allowed us to affirm that the MPF ruptured at surface with a decimetric offset during historical times, between 2.5 ka and 7th-8th cent. A.D. [for details see Galli *et al.* (2010)].

4. Conclusion

In this work, we present the results of the first high-resolution subsurface resistivity investigation carried out across the Paganica fault, which is the central segment of the seismogenic structure responsible for the April 6, 2009 earthquake (i.e., the Paganica-San Demetrio fault system).

ERT results were “calibrated” and correlated with data gathered through aerial photo interpretation, field geological investigation and four borehole logs, according to the morphological and stratigraphical framework defined in Galli *et al.* (2010). By comparing and matching all these data, we succeed in identifying the Paganica fault geometries both at depth, where it affects the limestone basement, and close to the surface, where it cuts across the Pleistocene-Holocene sediments. In particular, our investigations put in evidence the fact that the Paganica fault structure consists of at least three main splays (UPF, MPF and LPF), arranged in a staircase, normal fault geometry in the Paganica village area. These splays affect the paleo-Raiale alluvial fan sequence, and throw the deposits down SW-wards, below the present alluvial

plain.

On the whole, the electrical images proved to be useful in:

- 1) providing robust interpretation to the “supposed” fault scarp observed at site ERT2;
- 2) detecting and pinpointing fault location;
- 3) estimating the cumulative displacement and;
- 4) characterizing the structure of the fault zone.

The very-high resolution ERT4 has also allowed us to put in evidence the internal architecture of the MPF splay, giving valuable support for the siting of the paleoseismological trench performed successfully by Galli *et al.* (2010).

We think that the combined geophysical/geological approach presented in this study might aid in filling another small gap in the grasp of the L'Aquila region seismotectonics, providing new basic data to be used in seismic hazard assessment of the area.

Acknowledgments. The authors are deeply indebted to Kris Vanneste, whose criticisms strongly enhanced a previous version of this paper, and another anonymous referee. This paper was presented at the 28th GNGTS (Gruppo Nazionale di Geofisica della Terra Solida) National Meeting (November 16-19, 2009).

REFERENCES

- Boncio P., Lavecchia G. and Pace B.; 2004: *Defining a model of 3D seismogenic sources for seismic hazard assessment applications: the case of central Apennines (Italy)*. J. Seismol., **8**, 407-425.
- Boncio P., Pizzi A., Brozzetti F., Pomposo G., Lavecchia G., Di Naccio D. and Ferrarini F.; 2010: *Coseismic ground deformation of the 6 April 2009 L'Aquila earthquake (central Italy, M_w 6.3)*. Geophys. Res. Lett., **37**, doi: 10.1029/2010GL042807.
- Bosi C.; 1975: *Osservazioni preliminari su faglie probabilmente attive nell'Appennino centrale*. Boll. Soc. Geol. It., **94**, 827-859.
- Caputo R., Piscitelli S., Oliveto A., Rizzo E. and Lapenna V.; 2003: *The use of electrical resistivity tomographies in active tectonics: examples from the Tyrnavos Basin, Greece*. J. Geodyn., **36**, 19-35.
- Caputo R., Salviulo L., Piscitelli S. and Loperte A.; 2007: *Late Quaternary activity along the Scorciabuoi Fault (Southern Italy) as inferred from electrical resistivity tomographies*. Ann. Geophys., **50**, 213-224.
- Cirella A., Piatanesi A., Cocco M., Tinti E., Scognamiglio L., Michelini A., Lomax A. and Boschi E.; 2009: *Rupture history of the 2009 L'Aquila (Italy) earthquake from non-linear joint inversion of strong motion and GPS data*. Geophys. Res. Lett., **36**, L19304.
- Demagnet D., Renardy F., Vanneste K., Jongmans D., Camelbeeck T. and Meghraoui M.; 2001: *The use of geophysical prospecting for imaging active faults in the Roer Graben, Belgium*. Geophysics, **66**, 78-89.
- Diaferia I., Barchi M., Loddo M., Schiavone D. and Siniscalchi A.; 2006: *Detailed imaging of tectonic structures by multiscale earth resistivity tomographies: the Colfiorito normal faults (Central Italy)*. Geophys. Res. Lett., **33**, L09305, doi: 10.1029/2006GL025828.
- Falcucci E., Gori S., Peronace E., Fubelli G., Moro M., Saroli M., Giaccio B., Messina P., Naso G., Scardia G., Sposato A., Voltaggio M., Galli P. and Galadini F.; 2009: *The Paganica fault and surface coseismic ruptures caused by the 6 April 2009 earthquake (L'Aquila, central Italy)*. Seismol. Res. Lett., **80**, 940-950.
- Galadini F. and Galli P.; 2000: *Active tectonics in the central Apennines (Italy) - input data for seismic hazard assessment*. Nat. Hazards, **22**, 225-270.
- Galli P., Bosi V., Piscitelli S., Giocoli A. and Scionti V.; 2006: *Late Holocene earthquakes in southern Apennines:*

- paleoseismology of the Caggiano fault*. Int. J. Earth Sci., **95**, doi: 10.1007/s00531-005-0066-2.
- Galli P., Camassi R., Azzaro R., Bernardini F., Castenetto S., Molin D., Peronace E., Rossi A., Vecchi M. and Tertulliani A.; 2009: *Il terremoto aquilano del 6 aprile 2009: rilievo macrosismico, effetti di superficie ed implicazioni sismotettoniche*. Il Quaternario, **22**, 235-246.
- Galli P., Giaccio B. and Messina P.; 2010: *The 2009 central Italy earthquake seen through 0.5 Myr-long tectonic history of the L'Aquila faults system*. Quaternary Sci. Rev., doi: 10.1016/j.quascirev.2010.08.018.
- Giano S.I., Lapenna V., Piscitelli S. and Schiattarella M.; 2000: *Electrical imaging and self-potential surveys to study the geological setting of the Quaternary slope deposits in the Agri high valley (Southern Italy)*. Ann. Geofis., **43**, 409-419.
- Giocoli A., Burrato P., Galli P., Lapenna V., Piscitelli S., Rizzo E., Romano G., Siniscalchi A., Magri C. and Vannoli P.; 2008a: *Using the ERT method in tectonically active areas: hints from Southern Apennine (Italy)*. Adv. Geosci., **19**, 61-65.
- Giocoli A., Magri C., Vannoli P., Piscitelli S., Rizzo E., Siniscalchi A., Burrato P., Basso C. and Di Nocera S.; 2008b: *Electrical Resistivity Tomography investigations in the Ufita Valley (Southern Italy)*. Ann. Geophys., **51**, 213-223.
- Improta L., Ferranti L., De Martini P.M., Piscitelli S., Bruno P.P., Burrato P., Civico R., Giocoli A., Iorio M., D'Addezio G. and Maschio L.; 2010: *Detecting young, slow-slipping active faults by geologic and multidisciplinary high-resolution geophysical investigations: a case study from the Apennine seismic belt, Italy*. J. Geophys. Res. - Solid Earth, **115**, B11307, doi: 10.1029/2010JB000871.
- Loke M.H.; 2001: *Tutorial: 2-D and 3-D electrical imaging surveys*. In: Course notes for USGS workshop "2-D and 3-D inversion and modeling of surface and borehole resistivity data", Storrs, CT, 13-16 March 2001.
- Messina P., Galli P., Falcucci E., Galadini F., Giaccio B., Gori S., Peronace E. and Sposato A.; 2009a: *Evoluzione geologica e tettonica quaternaria dell'area interessata dal terremoto aquilano del 2009*. Geitalia, **28**, 24-29.
- Messina P., Galli P., Giaccio B. and Peronace E.; 2009b: *Quaternary tectonic evolution of the area affected by the Paganica fault (2009 L'Aquila earthquake)*. In: 28° GNGTS (Gruppo Nazionale di Geofisica della Terra Solida) National Meeting, November 16-19, 2009, pp. 47-50.
- Nguyen F., Garambois S., Jongmans D., Pirard E. and Loke M.H.; 2005: *Image processing of 2D resistivity data for imaging faults*. J. Appl. Geophys., **57**, 260-277.
- Pondrelli S., Salimbeni S., Morelli A., Ekström G., Olivieri M. and Boschi E.; 2009: *Seismic moment tensors of the April 2009, L'Aquila (Central Italy)*. Geophys. J. Int., **180**, 238-242.
- Rizzo E., Colella A., Lapenna V. and Piscitelli S.; 2004: *High-resolution imaging of the fault-controlled High Agri Valley basin (Southern Italy) with deep and shallow electrical resistivity tomographies*. Phys. Chem. Earth, **29**, 321-327.
- Siniscalchi A., Tripaldi S., Neri M., Giammanco S., Piscitelli S., Balasco M., Behncke B., Magri C., Naudet V. and Rizzo E.; 2010: *Insights into fluid circulation across the Pernicana Fault (Mt. Etna, Italy) and implications for flank instability*. J. Volcanol. Geotherm. Res., **193**, 137-142, doi: 10.1016/j.jvolgeores.2010.03.013.
- Storz H., Storz W. and Jacobs F.; 2000: *Electrical resistivity tomography to investigate geological structures of the Earth's upper crust*. Geophys. Prospect., **48**, 455-471.
- Suzuki K., Toda S., Kusunoki K., Fujimitsu Y., Mogi T. and Jomori A.; 2000: *Case studies of electrical and electromagnetic methods applied to mapping active faults beneath the thick quaternary*. Eng. Geol., **56**, 29-45.
- Wise D.J., Cassidy J. and Locke C.A.; 2003: *Geophysical imaging of the Quaternary Wairoa North Fault, New Zealand: a case study*. J. Appl. Geophys., **53**, 1-16.

Corresponding author: Alessandro Giocoli
Institute of Methodologies for Environmental Analysis IMAA-CNR
C/da S. Loja, 85050 Tito, (Potenza), Italy
Phone: +39 0971 427400; fax: +39 0971 427271; e-mail: giocoli@imaa.cnr.it